JCTC Journal of Chemical Theory and Computation

Article

pubs.acs.org/JCTC

Extensions of the Time-Dependent Density Functional Based Tight-Binding Approach

A. Domínguez,*[,†] B. Aradi,[†] T. Frauenheim,[†] V. Lutsker,[‡] and T. A. Niehaus[‡]

[†]Bremen Center for Computational Materials Science, Universität Bremen, Am Fallturm 1, 28359 Bremen, Germany

[‡]Department of Theoretical Physics, University of Regensburg, 93040 Regensburg, Germany

Supporting Information

ABSTRACT: The time-dependent density functional based tight-binding (TD-DFTB) approach is generalized to account for fractional occupations. In addition, an on-site correction leads to marked qualitative and quantitative improvements over the original method. Especially, the known failure of TD-DFTB for the description of $\sigma \rightarrow \pi^*$ and $n \rightarrow \pi^*$ excitations is overcome. Benchmark calculations on a large set of organic molecules also indicate a better description of triplet states. The accuracy of the revised TD-DFTB method is found to be similar to first principles TD-DFT calculations at a highly reduced computational cost. As a side issue, we also discuss the generalization of the TD-DFTB method to spin-polarized systems. In contrast to an earlier study, we obtain a formalism that is fully consistent with the use of local exchange-correlation functionals in the ground state DFTB method.

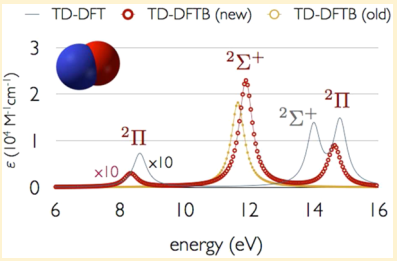

1. INTRODUCTION

During the last years, Density Functional Theory (DFT) has been one of the most utilized tools for the description of ground-state properties of a wide variety of molecular systems that range from small molecules to large periodic materials. While it lacks the accuracy typical of correlated wave function-based methods, it goes beyond Hartree−Fock (HF) as electron correlation is incorporated in a self-consistent-field (SCF) fashion. Thus, DFT has turned out to be a good compromise between accuracy and computational cost; affordable to study hundreds-of-atoms systems on most of the current workstations with fairly good precision. The field of application of this method was subsequently extended to the study of excited states properties with the development of time-dependent density functional theory (TD-DFT).[1] This method has become the de facto standard for the computation of optical properties for molecules with several tens of atoms. Also, the limitations of TD-DFT are now well documented in the literature (see, for example, refs 2−4), which together with benchmark data,[5−7] helps researchers to judge a priori whether a certain class of exchange-correlation (XC) functionals is sufficient for the predictive simulation of the problem at hand.

Still, many applications in photochemistry and nanophysics are not easily tractable in the current methodological frame. As an example, quantum molecular dynamics in the excited state require the evaluation of energies and forces at a large number of points along the trajectory. Also, the investigation of extended nanostructures such as nanowires and nanotubes with intrinsic defects or surface modifications can not be reliably performed with small models. For these kind of problems, an approximate TD-DFT method might be advantageous. Such a scheme is the time-dependent density functional based tight-binding method (TD-DFTB).[8] In the TD-DFTB method additional approximations beyond the choice of a given XC functional are performed to enhance the numerical efficiency. These are mostly the neglect and simplification of two-electron integrals occurring in the linear response formulation of TD-DFT. In contrast to HF-based semiempirical methods (such as INDO/S or CIS-PM3), TD-DFTB approximates a reference method that already covers electronic correlation to some degree and does not include free parameters that are adjusted to reproduce experimental data.

After the original linear response implementation,[8] TD-DFTB was extended in a number of different directions. Analytical excited state gradients have been derived,[9] as well as a real time propagation of Kohn−Sham (KS) orbitals that enables the computation of optical spectra using order-N algorithms.[10] Several groups worked on nonadiabatic molecular dynamics simulations in the Ehrenfest[11] or surface hopping[12,13] approach. More recent developments include a TD-DFTB approach for open boundary conditions in the field of quantum transport,[14] as well as an implementation for open shell systems.[15] A detailed review that summarizes advantages and limits of the method is also available.[16]

One of these limits is the rather poor description of $\sigma \rightarrow \pi^*$ and $n \rightarrow \pi^*$ excitations in many chromophores. In TD-DFTB these transitions show vanishing oscillator strengths although higher levels of theory clearly predict a finite (albeit small) transition probability. Moreover, singlet−triplet gaps for these kind of excitations are exactly zero in TD-DFTB, which is again in disagreement with more accurate methods. Although $\pi \rightarrow \pi^*$ transitions usually dominate the absorption spectrum, such low-lying excitations may play a significant role in the luminescence

Received: February 15, 2013
Published: September 27, 2013

   dx.doi.org/10.1021/ct400123t | J. Chem. Theory Comput. 2013, 9, 4901−4914

properties that are of key importance in many technological applications.

In this paper, we present extensions of the TD-DFTB method in order to improve its description of the absorption spectra of molecules. In section 1, the spin-unrestricted DFTB formulation for the ground state is briefly reviewed. Afterward, we generalize the TD-DFTB approach for the study of open-shell systems with fractional occupancy. In section 4, a refinement to overcome important deficiencies within the method is formulated. In order to highlight the qualitative improvement due to these extensions, we report results for selected diatomic molecules in section 5. Additionally, a comparison between results obtained with the proposed formalism and the original TD-DFTB approach for a large set of benchmark molecules is presented. Our findings are further compared to TD-DFT, the best theoretical estimates from the literature and experimental observations.

2. SPIN-UNRESTRICTED DFTB FOR THE GROUND STATE

This section contains a brief summary of the spin-unrestricted DFTB method in order to establish the required notation for the later parts. More details on the derivation and application of the method are given in the original article by Köhler and co-workers.[17]

DFTB is based on a expansion of the DFT-KS energy up to the second order in the charge density fluctuations, $\delta\rho = \delta\rho_\uparrow + \delta\rho_\downarrow$, around a reference density, $\rho_0 = [\rho_{0\uparrow}, \rho_{0\downarrow}]$. The latter is given by a superposition of precalculated densities for neutral spin-unpolarized atoms. The DFTB energy reads:

$$E = \sum_\sigma \sum_i n_{i\sigma}\langle\psi_{i\sigma}|\hat{H}^0|\psi_{i\sigma}\rangle + \frac{1}{2}\sum_{\sigma\tau}\int\int \delta\rho_\sigma(\mathbf{r}) \times f^{\mathrm{hxc}}_{\rho_\sigma\rho_\tau}[\rho_0](\mathbf{r},\mathbf{r}')\delta\rho_\tau(\mathbf{r}')\mathrm{d}\mathbf{r}\mathrm{d}\mathbf{r}' + E_{\mathrm{rep}} \tag{1}$$

where the $n_i\sigma$ denote occupation numbers, E_{rep} is a sum of pair potentials independent of the electronic density,[18] and $f^{\mathrm{hxc}} = f^{\mathrm{h}} + f^{\mathrm{xc}}$ with

$$f^{\mathrm{h}}(\mathbf{r},\mathbf{r}') = \frac{1}{|\mathbf{r}-\mathbf{r}'|}$$
$$f^{\mathrm{xc}}_{\rho_\sigma\rho_\tau}[\rho](\mathbf{r},\mathbf{r}') = \frac{\delta^2 E_{xc}[\rho]}{\delta\rho_\sigma(\mathbf{r})\delta\rho_\tau(\mathbf{r}')} \tag{2}$$

denote the Coulomb and XC kernel, respectively.

In the first (zeroth-order) term of eq 1, $\hat{H}^0$ is the KS Hamiltonian evaluated at ρ_0 and the sum runs over the spin variables $\sigma = \uparrow,\downarrow$ and the KS orbitals $\psi_{i\sigma}$. For the succeeding formulation, the Roman indices s, t, u, v, denote KS orbitals, whereas Greek indices $\mu, \nu, \kappa, \lambda$ will denote atomic orbitals (AO). Let us also abbreviate a general two-point integral over a kernel $g(\mathbf{r},\mathbf{r}')$ in the following form:

$$(f|g|h) = \int\int f(\mathbf{r})g(\mathbf{r},\mathbf{r}')h(\mathbf{r}')\mathrm{d}\mathbf{r}\,\mathrm{d}\mathbf{r}' \tag{3}$$

For atomic orbital products $f(\mathbf{r}) = \phi_\mu(\mathbf{r})\phi_\nu(\mathbf{r})$ and $h(\mathbf{r}') = \phi_\kappa(\mathbf{r}')\phi_\lambda(\mathbf{r}')$ the shorthand $(\mu\nu|g|\kappa\lambda)$ will be also used. Expanding the KS orbitals (which we choose to be real) into a suitable set of such localized atom-centered AO, $\psi_{i\sigma} = \Sigma_\mu C^\sigma_{\mu i}\phi_\mu$, the second term in eq 1, labeled $E^{(2)}$ in the following, can be written as

$$E^{(2)} = \frac{1}{2}\sum_{\sigma\tau}\sum_{\mu\nu\kappa\lambda}\Delta P^\sigma_{\mu\nu}(\mu\nu|f^{\mathrm{hxc}}_{\rho_\sigma\rho_\tau}[\rho_0]|\kappa\lambda)\Delta P^\tau_{\kappa\lambda} \tag{4}$$

where $\Delta P^\sigma_{\mu\nu} = P^\sigma_{\mu\nu} - P^{0,\sigma}_{\mu\nu}$ denotes the AO density matrix of the difference density $\delta\rho_\sigma(\mathbf{r})$, with

$$P^\sigma_{\mu\nu} = \sum_{st} c^\sigma_{\mu s}P^\sigma_{st}c^\sigma_{\nu t},\ P^{0,\sigma}_{\mu\nu} = \sum_{st} c^\sigma_{\mu s}P^{0,\sigma}_{st}c^\sigma_{\nu t} \tag{5}$$

Here, $P^\sigma_{st} = \langle\Psi|\hat{a}^\dagger_{t\sigma}\hat{a}_{s\sigma}|\Psi\rangle$ are the MO density matrix elements, Ψ being the ground state KS determinant. The term $P^{0,\sigma}_{st}$ designates the MO density matrix of the reference system.

To evaluate the appearing integrals, the Mulliken approximation is applied. This amounts to set $\phi_\mu\phi_\nu \approx {}^1/_2 S_{\mu\nu}(|\phi_\mu|^2 + |\phi_\nu|^2)$, using the known AO overlap integrals $S_{\mu\nu}$. Thus, the general four-center integrals are written in terms of two-center integrals,

$$(\mu\nu|f^{\mathrm{hxc}}_{\rho_\sigma\rho_\tau}[\rho_0]|\kappa\lambda) \approx \frac{1}{4}S_{\mu\nu}S_{\kappa\lambda}\sum_{\alpha\in\{\mu,\nu\}}\sum_{\beta\in\{\kappa,\lambda\}}(\alpha\alpha|f^{\mathrm{hxc}}_{\rho_\sigma\rho_\tau}[\rho_0]|\beta\beta) \tag{6}$$

By substituting eq 6 into eq 4, the second order contribution to the energy reads,

$$E^{(2)} = \frac{1}{2}\sum_{\sigma\tau}\sum_{\mu\nu}\Delta\tilde{P}^\sigma_{\mu\mu}(\mu\mu|f^{\mathrm{hxc}}_{\rho_\sigma\rho_\tau}[\rho_0]|\nu\nu)\Delta\tilde{P}^\tau_{\nu\nu} \tag{7}$$

where $\tilde{P}^\sigma_{\mu\nu}$ are the elements of the dual density matrix defined as

$$\tilde{\mathbf{P}}^\sigma = \frac{1}{2}(\mathbf{P}^\sigma\mathbf{S} + \mathbf{S}\mathbf{P}^\sigma) \tag{8}$$

The concept of a dual representation of the density matrix was introduced by Han et al. in their implementation of the LDA + U method.[19] The authors show that for a nonorthogonal orbital basis this matrix satisfies exactly the sum rule, $\Sigma_\sigma\mathrm{Tr}(\tilde{\mathbf{P}}^\sigma) = N_e$, where N_e is the total number of electrons. They also pointed out, that the use of the dual density matrix is consistent with the Mulliken population analysis.

By using eq 5, the dual density matrix can be expressed with respect to the MO density matrix as

$$\tilde{P}^\sigma_{\mu\nu} = \sum_{st}\tilde{P}^{st\sigma}_{\mu\nu}P^\sigma_{st} \tag{9}$$

where the matrix $\tilde{\mathbf{P}}^{st\sigma}$ is defined as follows:

$$\tilde{P}^{st\sigma}_{\mu\nu} = \frac{1}{4}(c^\sigma_{\mu s}\tilde{c}^\sigma_{\nu t} + c^\sigma_{\mu t}\tilde{c}^\sigma_{\nu s} + c^\sigma_{\nu s}\tilde{c}^\sigma_{\mu t} + c^\sigma_{\nu t}\tilde{c}^\sigma_{\mu s}),\quad \tilde{\mathbf{c}}_s = \mathbf{c}_s\mathbf{S} \tag{10}$$

A further simplification to eq 7 is obtained by spherical averaging over AO products. This ensures that the final total energy expression is invariant with respect to arbitrary rotations of the molecular frame. To this end, the functions F_{Al} are introduced

$$F_{Al}(|r-\mathbf{R}_A|) = \frac{1}{2l+1}\sum_{m=-l}^{m=l}|\phi_\mu(r-\mathbf{R}_A)|^2 \tag{11}$$

where l and m denote the angular momentum and magnetic quantum number of AO ϕ_μ, centered on atom A. We then have for $\mu = \{Alm\}$, $\nu = \{Bl'm'\}$:

$$(\mu\mu|f^{\mathrm{hxc}}_{\rho_\sigma\rho_\tau}[\rho_0]|\nu\nu) \approx (F_{Al}|f^{\mathrm{hxc}}_{\rho_\sigma\rho_\tau}[\rho_0]|F_{Bl'}) = \Gamma^{\sigma\tau}_{Al,Bl'} \tag{12}$$

introducing the shorthand notation Γ.

dx.doi.org/10.1021/ct400123t | J. Chem. Theory Comput. 2013, 9, 4901−4914

The traditional DFTB energy expression is now obtained after transformation from the set $\{\rho_\uparrow,\rho_\downarrow\}$ to the total density $\rho = \rho_\uparrow + \rho_\downarrow$ and magnetization $m = \rho_\uparrow - \rho_\downarrow$. By this change of variables, the XC kernel can be split and one arrives at (see Appendix A)

$$\Gamma^{\sigma\tau}_{Al,Bl'} = \gamma_{Al,Bl'} + \delta_\sigma\delta_\tau\delta_{AB}W_{Al,l'} \tag{13}$$

where $\delta_\sigma = 2\delta_{\sigma\uparrow}-1$ and the parameters $\gamma_{Al,Bl'} = (F_{Al}|f^{hxc}_{\rho\rho}[\rho_0]|F_{Bl'})$ and $W_{Al,l'} = (F_{Al}|f^{xc}_{mm}[\rho_0]|F_{Al'})$. Please note that the constants $W_{Al,l'}$ depend only on the XC kernel but not on the long-range Coulomb interaction. Moreover, as the reference density ρ_0 is built from neutral spin-unpolarized atomic densities and the XC functional is an even functional in m, there are no integrals, which involve mixed derivatives of the XC energy with respect to both density and magnetization. The parameters $\gamma_{Al,Bl'}$ and $W_{Al,l'}$ are known in the DFTB method as the γ-functional and spin coupling constants, respectively.[18] The spin coupling constants are treated as strictly on-site parameters, whereas γ is calculated for every atom pair using an interpolation formula, which depends on the distance between the atoms A and B and the atomic Hubbard-like parameters $\gamma_{Al,Al}$ and $\gamma_{Bl,Bl}$. Traditionally, the latter are not computed directly from the integral eq 12 but from total energy derivatives according to $\gamma_{Al,Al} = \delta^2E/\delta n^2$. In this expression, E denotes the DFT total energy of atom A and n refers to the occupation of the shell with angular momentum l. The derivative is then evaluated numerically by full self-consistent field calculations at perturbed occupations. Due to orbital relaxation, parameters obtained in this way are roughly 10−20% smaller than the ones from a direct integral evaluation. This point will become important later.

Finally, by substituting eq 9 in eq 7 while using eq 12, the second order energy term can be expressed as

$$E^{(2)} = \frac{1}{2}\sum_{\sigma\tau}\sum_{stuv}\sum_{ABll'}\Delta P^\sigma_{st}q^{st\sigma}_{Al}\Gamma^{\sigma\tau}_{Al,Bl'}q^{uv\tau}_{Bl'}\Delta P^\tau_{uv} \tag{14}$$

where $\Delta P^\sigma_{st} = P^\sigma_{st} - P^{0,\sigma}_{st}$ and $q^{st\sigma}_{Al} = \Sigma_{\mu\in A,l}\tilde{P}^{st\sigma}_{\mu\mu}$. For later reference, we next define a matrix $\overline{\mathbf{K}}$:

$$\overline{K}_{st\sigma,uv\tau} = \sum_{ABll'} q^{st\sigma}_{Al}\Gamma^{\sigma\tau}_{Al,Bl'}q^{uv\tau}_{Bl'} \tag{15}$$

Using this abbreviation, the DFTB total energy can then be written in the following simple form,

$$E = \sum_\sigma\sum_{st}H^0_{st\sigma}P^\sigma_{st} + \frac{1}{2}\sum_{\sigma\tau}\sum_{stuv}\Delta P^\sigma_{st}\overline{K}_{st\sigma,uv\tau}\Delta P^\tau_{uv} + E_{\mathrm{rep}} \tag{16}$$

By applying the variational principle to the energy functional, the DFTB KS equations are obtained

$$H_{st\sigma} - \varepsilon_{s\sigma}\delta_{st} = 0, \quad \forall\ s, t, \sigma \tag{17}$$

where the KS Hamiltonian is expressed as

$$H_{st\sigma} = \frac{\partial E}{\partial P^\sigma_{st}} = H^0_{st\sigma} + \sum_\tau\sum_{uv}\overline{K}_{st\sigma,uv\tau}\Delta P^\tau_{uv} \tag{18}$$

These equations are subsequently transformed into a set of algebraic equations by expanding the KS orbitals into the AO basis and are solved self-consistently. For the converged ground state density, we have $P^\sigma_{st} = n_{s\sigma}\delta_{st}$. Using also the identity $\Sigma_{st}c^\sigma_{\mu s}P^{0,\sigma}_{st}c^\sigma_{vt} = n^0_{\mu\sigma}\delta_{\mu\nu}(\forall\mu, \nu, \sigma)$, $n^0_{\mu\sigma}$ being the occupation numbers for the reference atoms, it is straightforward to recover the expression for the spin-unrestricted DFTB Hamiltonian given in refs 17 and 18 (see Appendix B for more details).

We would like to emphasize that unlike the original formulation of DFTB, the energy functional and the KS Hamiltonian are expressed here in terms of the KS density matrix fluctuations. This more general formalism will be suitable for the succeeding derivation of the TD-DFTB method and its further extension.

3. SPIN-UNRESTRICTED TD-DFTB

Once the KS orbitals $\psi_{i\sigma}$ and energies $\varepsilon_{i\sigma}$ are obtained, a linear density-response treatment directly applies as a natural extension to DFTB. Following Casida,[20] the excitation energies ω_I and eigenvectors F_I can be calculated by solving the eigenvalue problem

$$\mathbf{\Omega F}_I = \omega_I^2\mathbf{F}_I \tag{19}$$

where the response matrix $\mathbf{\Omega}$ is defined as

$$\Omega = \mathbf{S}^{-1/2}(\mathbf{A} + \mathbf{B})\mathbf{S}^{-1/2} \tag{20}$$

$$\mathbf{S} = -\mathbf{C}(\mathbf{A} - \mathbf{B})^{-1}\mathbf{C} \tag{21}$$

The matrices $\boldsymbol{A}$, $\boldsymbol{B}$, and $\boldsymbol{C}$ are defined according to

$$\begin{aligned}\boldsymbol{A}_{ia\sigma,jb\tau} &= \frac{\delta_{ij}\delta_{ab}\delta_{\sigma\tau}\omega_{jb\tau}}{n_{j\tau} - n_{b\tau}} + K_{ia\sigma,jb\tau}\\ \boldsymbol{B}_{ia\sigma,jb\tau} &= K_{ia\sigma,bj\tau}\\ \boldsymbol{C}_{ia\sigma,jb\tau} &= \frac{\delta_{ij}\delta_{ab}\delta_{\sigma\tau}}{n_{j\tau} - n_{b\tau}}\end{aligned} \tag{22}$$

where $\omega_{jb\tau} = \varepsilon_{b\tau} - \varepsilon_{j\tau}$ and the indexes i, j, a, b stand for KS orbitals such that $n_{i\sigma} > n_{a\sigma}$ and $n_{j\tau} > n_{b\tau}$. We explicitly allow for fractional occupations at this point in order to be able to simulate also metallic or near-metallic systems at elevated electronic temperature.

The coupling matrix elements $K_{ia\sigma,jb\tau}$ are generally defined as the derivative of the KS Hamiltonian with respect to the density matrix elements. For the special case of DFTB (see eq 18), this leads to the matrix $\overline{\mathbf{K}}$ defined in eq 15

$$K_{ia\sigma,jb\tau}: = \frac{\partial H_{ia\sigma}}{\partial P^\tau_{jb}} = \overline{K}_{ia\sigma,jb\tau} \tag{23}$$

This quantity depends only on the γ and W parameters, as well as on $q^{st\sigma}_{Al}$, introduced in eq 15. In this case, for which $s = i$ and $t = a$, the quantities, $q^{ia\sigma}_{Al}$, are called Mulliken transition charges[8] and the matrix $\tilde{\mathbf{P}}^{ia\sigma}$, defined in eq 10, represents the dual KS transition density for an excitation from orbital i to a. The Mulliken transition charges are obtained from the previous ground state DFTB calculation.

An important feature of the coupling matrix for local or semilocal XC functionals is its invariance with respect to the permutation of any connected (real orbital) indices (e.g., $K_{ia\sigma,jb\tau} = K_{ia\sigma,bj\tau} = K_{ai\sigma,jb\tau}$). This symmetry does not hold for functionals involving Hartree−Fock exchange.[20] In contrast to an earlier derivation by Traniet et al.,[15] we find that the DFTB coupling matrix is in fact symmetric. This can be traced back to the dual transition density matrix, eq 10, that evidently has this property. Since the ground state DFTB method is derived as an approximation to local or semilocal DFT only,[21] this is an expected and necessary property and implies that the orbital rotation Hessian $\mathbf{A} - \mathbf{B}$ becomes strictly diagonal. This is not the case in ref 15 where the authors obtain a nondiagonal $\mathbf{A} - \mathbf{B}$

dx.doi.org/10.1021/ct400123t | J. Chem. Theory Comput. 2013, 9, 4901−4914

matrix. They claim, however, that the antisymmetric component of the coupling matrix has a rather small effect on their results, which are similar to original TD-DFTB findings.

Due to the symmetry of the coupling matrix, the expression for the response matrix elements is conveniently simplified to read

$$\Omega_{ia\sigma,jb\tau} = \delta_{ij}\delta_{ab}\delta_{\sigma\tau}\omega^2_{jb\tau} + 2\sqrt{(n_{i\sigma} - n_{a\sigma})\omega_{ia\sigma}}K_{ia\sigma,jb\tau}\sqrt{(n_{j\tau} - n_{b\tau})\omega_{jb\tau}} \tag{24}$$

It is worth formulating the method for closed shell systems as a particular case, in order to make contact with the original derivation of TD-DFTB. In this special case, the Mulliken transition charges have the property $q^{ia\uparrow}_{Al} = q^{ia\downarrow}_{Al} = q^{ia}_{Al}$. If, in addition, the dependence of the γ-functional and W constants on the angular momentum is neglected, the coupling matrix simplifies to

$$K_{ia\sigma,jb\tau} = \sum_{AB} q^{ia}_A(\gamma_{AB} + \delta_\sigma\delta_\tau\delta_{AB}W_A)q^{jb}_B \tag{25}$$

with $q^{ia}_A = \Sigma_l q^{ia}_{Al}$, in full agreement[22] with the expression derived previously for spin-unpolarized densities.[8]

Once the eigenvalue problem is solved within TD-DFTB, the oscillator strength related to excitation I can be calculated as

$$f^I = \frac{2}{3}\sum_{k=1}^{3}\left|\sum_{ia\sigma}\langle\psi_{i\sigma}|\hat{r}_k|\psi_{a\sigma}\rangle\sqrt{(n_{i\sigma} - n_{a\sigma})\omega_{ia\sigma}}F^I_{ia\sigma}\right|^2 \tag{26}$$

where $\hat{r}_k$ denotes the k-th component of the position operator. The transition-dipole matrix elements are also subjected to a Mulliken approximation ($\mathbf{R}_A$ is the position of atom A):

$$\langle\psi_{i\sigma}|\hat{\mathbf{r}}|\psi_{a\sigma}\rangle \approx \sum_A \mathbf{R}_A q^{ia\sigma}_A \tag{27}$$

4. BEYOND THE MULLIKEN APPROXIMATION

While in general the Mulliken approximation accounts, at least approximately, for the differential overlap of atomic orbitals, there is an important exception. If orbitals ϕ_μ and ϕ_ν with $\mu \neq \nu$ reside on the same atom, their product vanishes since the overlap matrix reduces to the identity. As a consequence, the transition charges are underestimated or often vanish identically for excitations that feature localized MO (e.g., $n \rightarrow \pi^*$ transitions). This in turn means that the coupling matrix vanishes and hence no correction of the ground state KS energy differences occurs in the linear response treatment. More importantly, the singlet−triplet gap is zero for such excitations.

A next level of approximation demands therefore the evaluation of all one-center integrals of the exchange type, that is, $(\mu\nu|f^{\mathrm{hxc}}_{\rho_\sigma\rho_\tau}[\rho_0]|\mu\nu)$ with $\mu \neq \nu$. This is how Pople et al. proceeded in the development of the intermediate neglect of differential overlap model (INDO)[23] to overcome the deficiencies encountered within the complete neglect of differential overlap method (CNDO).[24] Under the INDO model, the one-center, two-electron integrals are fitted to atomic spectroscopic data. In this work, the corresponding one-center integrals are calculated by numerical integration.

After inclusion of every onsite exchange-like integral within the DFTB formalism (see Appendix C), the second-order energy takes the new form:

$$\begin{aligned}E^{(2)} = &\frac{1}{2}\sum_{\sigma\tau}\sum_A\sum_{\mu\nu\in A}\Delta\tilde{P}^\sigma_{\mu\mu}(\mu\mu|f^{\mathrm{hxc}}_{\rho_\sigma\rho_\tau}[\rho_0]|\nu\nu)\Delta\tilde{P}^\tau_{\nu\nu}\\ &+\sum_{\sigma\tau}\sum_A\sum_{\mu\nu\in A}^{\mu\neq\nu}\Delta\tilde{P}^\sigma_{\mu\nu}(\mu\nu|f^{\mathrm{hxc}}_{\rho_\sigma\rho_\tau}[\rho_0]|\mu\nu)\Delta\tilde{P}^\tau_{\mu\nu}\\ &+\frac{1}{2}\sum_{\sigma\tau}\sum_{AB}^{A\neq B}\sum_{\mu\in A}\sum_{\nu\in B}\Delta\tilde{P}^\sigma_{\mu\mu}(\mu\mu|f^{\mathrm{hxc}}_{\rho_\sigma\rho_\tau}[\rho_0]|\nu\nu)\Delta\tilde{P}^\tau_{\nu\nu}\end{aligned} \tag{28}$$

where the onsite integrals appear in the second term and the previous energy expression (eq 7) has been split into on-site (first term) and off-site (third term) contributions.

By substituting eq 9 in eq 28 while using eq 12 for the off-site component, $E^{(2)}$ can be finally written as

$$E^{(2)} = \frac{1}{2}\sum_{\sigma\tau}\sum_{stuv}\Delta P^\sigma_{st}K_{st\sigma,uv\tau}\Delta P^\tau_{uv} \tag{29}$$

with the refined coupling matrix $\mathbf{K}$ being expressed as

$$\begin{aligned}K_{st\sigma,uv\tau} = &\sum_A\sum_{\mu\nu\in A}\tilde{P}^{st\sigma}_{\mu\mu}(\mu\mu|f^{\mathrm{hxc}}_{\rho_\sigma\rho_\tau}[\rho_0]|\nu\nu)\tilde{P}^{uv\tau}_{\nu\nu}\\ &+2\sum_A\sum_{\mu\nu\in A}^{\mu\neq\nu}\tilde{P}^{st\sigma}_{\mu\nu}(\mu\nu|f^{\mathrm{hxc}}_{\rho_\sigma\rho_\tau}[\rho_0]|\mu\nu)\tilde{P}^{uv\tau}_{\mu\nu}\\ &+\sum_{ABll'}^{A\neq B}q^{st\sigma}_{Al}\Gamma^{\sigma\tau}_{Al,Bl'}q^{uv\tau}_{Bl'}.\end{aligned} \tag{30}$$

With inclusion of the exchange integrals, the spherical averaging over AO products described in eq 12 will in general not lead to an expression, which is invariant under a rotation of the atomic axes. This has been discussed by Figeys et. al,[25] who analyzed the rotational invariance (RI) of the INDO model. Taking p-type orbitals as an example, the following identity must hold to preserve RI:

$$(pp|f^{\mathrm{hxc}}_{\rho_\sigma\rho_\tau}[\rho_0]|pp) - (pp|f^{\mathrm{hxc}}_{\rho_\sigma\rho_\tau}[\rho_0]|p'p') = 2(pp'|f^{\mathrm{hxc}}_{\rho_\sigma\rho_\tau}[\rho_0]|pp'),\ \forall\ p, p' \tag{31}$$

In the original DFTB formulation this requirement is fulfilled, as both integrals on the left-hand side of eq 31 are approximated to have the same value,$\Gamma^{\sigma\tau}_{Ap,Ap}$, while the integral on the right-hand side is neglected. To retain RI within the present scheme, one could evaluate all on-site integrals exactly so that eq 31 holds automatically. As detailed in section 2, the corresponding averaged Γ-parameters would then differ from the ones usually employed in ground state DFTB simulations, which are obtained from total energy derivatives. Instead, we use eq 31 to calculate all required parameters, taking the exact exchange integrals and the traditional Γ-parameters as input.[26] In this way, the modifications of the original method are kept as small as possible, while RI is still exactly preserved.

The eqs 29 and 30 represent a correction to the conventional DFTB energy expression, whose implication for various ground state properties certainly warrants a deeper investigation. Since we are mainly interested in an improvement of the TD-DFTB scheme at this point, we keep with the traditional DFTB scheme for the ground state and employ the modified coupling matrix only in the response part of the calculation, that is, in eq 22.

In a similar manner as the refinement of the coupling matrix was achieved, the approximation for the dipole matrix elements (eq 27), and hence the oscillator strength, can be improved by

Table 1. Comparison of Vertical Excitation Energies ω_I and Oscillator Strengths f_I for TD-DFT with TZP Basis Set, the Traditional TD-DFTB Method (Old) and TD-DFTB with Onsite Correction (New)[a]

	TD-DFT			TD-DFTB					
trans.	ω_I	f_I	ω_{KS}	ω_I^{new}	f_I^{new}	ω_I^{old}	f_I^{old}	ω_{KS}	exp.
				NO					
Σ^+ ($\pi \rightarrow \pi^*$)	6.46	<0.01	8.36	7.22	<0.01	7.49	<0.01	8.53	
II ($\sigma \rightarrow \pi^*$)	6.49	<0.01	7.23	7.29	<0.01	7.77	0.00	7.80/7.77	
Δ ($\pi \rightarrow \pi^*$)	7.26	0.00	8.36	7.74	0.00	8.53	0.00	8.64/8.53	
Σ^- ($\pi \rightarrow \pi^*$)	8.36	0.00	8.36	8.53	0.00	8.53	0.00	8.53	
^{2}II ($\sigma \rightarrow \pi^*$)	8.61	0.02	7.84	8.33	0.01	7.80	0.0	7.77/7.80	
Σ^- ($\pi \rightarrow \pi^*$)	8.74	0.00	8.74	8.64	0.00	8.64	0.00	8.64	
$^2\Delta$ ($\pi \rightarrow \pi^*$)	9.11	0.00	8.74	9.09	0.00	8.64	0.00	8.64	
II ($\sigma^* \rightarrow \pi^*$)	11.64	<0.01	12.45	12.68	<0.01	13.19	0.00	13.19	
$^2\Sigma^+$ ($\pi \rightarrow \pi^*$)	14.0	0.35	8.47	11.90	0.63	11.65	0.50	8.64	
^{2}II ($\sigma^* \rightarrow \pi^*$)	14.82	0.38	12.87	14.64	0.24	13.23	0.00	13.23	
				N_2					
$^3\Pi_g$ ($\sigma_g \rightarrow \pi_g$)	7.30		8.20	7.48		8.12		8.12	8.04
$^3\Sigma_u^+$ ($\pi_u \rightarrow \pi_g$)	7.42		9.60	6.91		7.36		9.01	7.75
$^3\Delta_u$ ($\pi_u \rightarrow \pi_g$)	8.24		9.60	7.76		9.01		9.01	8.88
$^3\Sigma_u^-$ ($\pi_u \rightarrow \pi_g$)	9.60		9.60	9.01		9.01		9.01	9.67
$^3\Pi_u$ ($\sigma_u \rightarrow \pi_g$)	10.37		11.49	11.30		12.06		12.06	11.19
$^1\Pi_g$ ($\sigma_g \rightarrow \pi_g$)	9.05	0.00	8.20	8.71	0.00	8.12	0.00	8.12	9.31
$^1\Sigma_u^-$ ($\pi_u \rightarrow \pi_g$)	9.60	0.00	9.60	9.01	0.00	9.01	0.00	9.01	9.92
$^1\Delta_u$ ($\pi_u \rightarrow \pi_g$)	10.03	0.00	9.60	9.66	0.00	9.01	0.00	9.01	10.27
$^1\Pi_u$ ($\sigma_u \rightarrow \pi_g$)	13.53	0.42	11.49	13.82	0.33	12.06	0.00	12.06	12.78
$^1\Sigma_u^+$ ($\pi_u \rightarrow \pi_g$)	14.84	0.77	9.60	13.02	0.98	12.75	0.80	9.01	12.96
				O_2					
$^3\Delta_u$ ($\pi_u \rightarrow \pi_g$)	6.39	0.00	6.90	6.21	0.00	6.35	0.00	6.35	6.0−6.2
$^3\Sigma_u^-$ ($\pi_u \rightarrow \pi_g$)	6.90	0.00	6.90	6.35	0.00	6.35	0.00	6.35	6.3−6.5
$^3\Pi_g$ ($\sigma_g \rightarrow \pi_g$)	7.84	0.00	7.91	6.80	0.00	6.79	0.00	6.79	
$^3\Sigma_u^+$ ($\pi_u \rightarrow \pi_g$)	9.00	0.18	6.90	8.36	0.32	8.21	0.24	6.35	∼8.6
$^3\Pi_u$ ($\sigma_u \rightarrow \pi_g$)	14.85	0.18	14.16	15.35	0.18	14.52	0.00	14.52	

[a]The PBE functional is used throughout. ω_{KS} denotes the KS orbital energy difference corresponding to the most dominant single particle transition in the many body wavefunction, as discussed by Casida in ref 20. Experimental data for N_2 and O_2 were taken from ref 33 and inferred from the potential energy curves in ref 34, respectively. Oscillator strengths are only provided for excitations that are not trivially spin-forbidden. All energies are expressed in eV.

including all nonvanishing one-center dipole integrals (see Appendix D),

$$\langle \psi_{i\sigma} | \hat{\mathbf{r}} | \psi_{a\sigma} \rangle = \sum_A \mathbf{R}_A q_A^{ia\sigma} + \sum_A \sum_{\mu\nu \in A}^{\mu \neq \nu} P_{\mu\nu}^{ia\sigma} \langle \mu | \hat{\mathbf{r}} | \nu \rangle \tag{32}$$

According to the dipole selection rules only $s-p$ and $p-d$ dipole integrals are nonzero. Among the $s-p$ integrals, only those of the type $D_{sp} = \langle s|r_k|p_k\rangle$ do not vanish, all of them being equal. With regards to the $p-d$ integrals, eleven of them are nonvanishing:

$$\begin{aligned} D_{pd} &= \langle p_y|x|d_{xy}\rangle = \langle p_x|y|d_{xy}\rangle = \langle p_y|z|d_{yz}\rangle = \langle p_z|y|d_{yz}\rangle \\ &= \langle p_z|x|d_{xz}\rangle = \langle p_x|z|d_{xz}\rangle \\ D_{pd} &= \langle p_x|x|d_{x^2-y^2}\rangle = -\langle p_y|y|d_{x^2-y^2}\rangle \\ D'_{pd} &= \langle p_y|y|d_{z^2}\rangle = \langle p_x|x|d_{z^2}\rangle \\ D''_{pd} &= \langle p_z|z|d_{z^2}\rangle \end{aligned} \tag{33}$$

We stress that the required additional atomic integrals in our correction to the coupling matrix and oscillator strength are neither freely adjustable parameters nor fitted to experiment. Instead, they are calculated numerically with a special-purpose DFT code that was recently developed in our group (for details on the evaluation of the onsite integrals, see Appendix E). As in earlier studies with the DFTB method, the Perdew−Burke−Ernzerhof (PBE)[27] functional was used in the calculation of Hamiltonian and overlap matrices, as well as the computation of reference densities and basis functions.[28] This also holds for the new parameters, which are calculated once for every atom type, stored in a file, and read when needed during the calculation. The presented extensions of the TD-DFTB method have been implemented in a development version of the DFTB+ code.[29]

5. RESULTS

5.1. Diatomic Molecules. To show the performance of our corrections to the coupling and dipole matrices (hereafter referred to as the onsite correction), we calculated the low-lying vertical excitation energies and their corresponding oscillator strengths of three diatomic molecules for which the improvements over traditional TD-DFTB are especially noticeable. It is important to point out that only valence excited states can be treated within TD-DFTB due to the employed minimal basis set. Table 1 shows the excitation energies of NO, N_2, and O_2 calculated within both the corrected and the original formulation

dx.doi.org/10.1021/ct400123t | J. Chem. Theory Comput. 2013, 9, 4901−4914

of TD-DFTB. For NO and O_2, spin-unrestricted TD-DFTB calculations have been performed, where doublet and triplet ground states have been considered, respectively. In order to identify the excited state multiplicity of the open-shell systems, the expectation value of the square of the total spin operator, $\langle S^2 \rangle$, is evaluated. We apply the expression II.83 in ref 30 for this purpose.[31] In Table 1, a multiplicity is only assigned to those excited states with low spin contamination. This covers the most important excitations in the absorption spectrum.

As a reference, we computed vertical excitation energies to valence states of these compounds by using TD-DFT as implemented in the TURBOMOLE package.[32] The PBE XC functional as well as triple-ζ plus polarization (TZP) basis set has been used. All ground state geometries were previously optimized at the corresponding level of theory. Some experimental findings taken from the literature are also included for comparison.[33,34] The oscillator strength for each excitation is indicated to the right of the corresponding excitation energy and in the first column of the table the symmetry and type of the transition is specified.

These molecules have as a common feature that they all possess low-lying $\sigma \rightarrow \pi^*$ excitations playing an important role in their absorption spectra. As stated above, a wrong description of these transitions is a known issue in current TD-DFTB. Below, we identify yet another failure in the description of some $\pi \rightarrow \pi^*$ transitions of these compounds.

NO belongs to the symmetry point group $C_{\infty v}$ for which Π and Σ^+ transitions are electric dipole allowed. However, TD-DFTB describes the former as forbidden. This is due to the mentioned vanishing of the corresponding transition charge, which leads to an equality of the KS energy difference ω_{KS} (termed $\omega_{jb\tau}$ in eq 22) and the excited state energy ω_I. Within the refined formulation this failure is successfully overcome as shown in Table 1. This improvement is specially important for the second and fourth Π transitions with oscillator strengths of 0.01 and 0.24, respectively, which are in agreement with the TD-DFT values of 0.02 and 0.38. Our correction is in this case, essential for providing qualitatively correct oscillator strengths in the absorption spectrum (see Figure 1) where traditional TD-DFTB is able to describe only the Σ^+ peak.

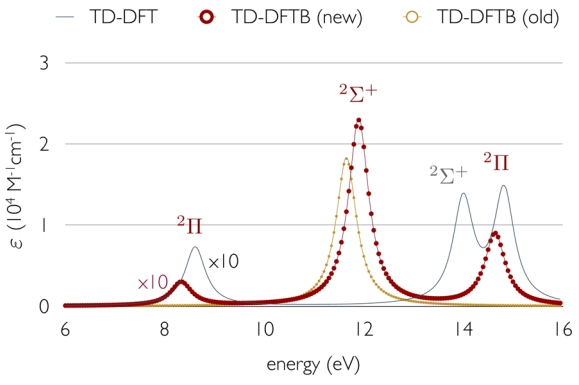

Figure 1. Absorption spectrum[35] of nitric oxide as obtained with full TD-DFT (PBE/TZP), traditional TD-DFTB (old), and TD-DFTB with on-site corrections (new).

The onsite correction also improves the description of Π transitions quantitatively. For example, the first Π excitation energy is clearly overestimated with respect to first-principle results. When using our correction the overestimation is reduced by almost 0.5 eV. Oppositely, the second Π excitation energy is strongly underestimated within traditional TD-DFTB whereas the corrected calculations return a value (8.33 eV) close to that from TD-DFT (8.61 eV). The Σ^+ ($\pi \rightarrow \pi^*$) transitions are also found to be better described within our correction, although the first (second) Σ^+ excitation energy is still significantly overestimated (underestimated). The Σ^- ($\pi \rightarrow \pi^*$) excitations energies are on the other hand unaffected by our correction. For these transitions no shift from their KS energy differences are seen, which agrees with first-principle observations. More importantly, the onsite correction rectifies the wrong degeneracy of the transitions Σ^- and Δ, which we identify as another important qualitative issue within traditional TD-DFTB. The correction also reduces the spin contamination of the doublet $^2\Pi$ states.

The electric-dipole-allowed transitions $^1\Pi_u$ and $^3\Pi_u$ of the homonuclear molecules N_2 and O_2 (point group $D_{\infty h}$), respectively, are neither correctly described by traditional TD-DFTB as shown in section 1. When applying the onsite correction, these excitations become allowed with oscillator strengths in agreement with ab initio results. However, it is necessary to indicate that the excitation energy of the latter transition is somewhat overestimated, being in better agreement within the non-corrected formalism. In contrast, the onsite correction greatly improves the agreement of the excitation energy of N_2 $^1\Pi_u$ with the TD-DFT result. This transition and the $^3\Pi_u$ state are degenerate according to traditional results whereas such degeneracy is broken at the corrected TD-DFTB level. This degeneracy breaking is in total correspondence with the results obtained at a higher level of theory.

The original formalism also predicts the degeneracy of the singlet and triplet Σ_u^- and Δ_u states of N_2 with excitation energy equal to 9.01 eV. This is, however, only partially confirmed by the ab initio results and in total disagreement with the experimental findings. According to TD-DFT, the triplet and singlet Σ_u^- states are degenerate with corresponding excitation energy of 9.60 eV but the triplet and singlet Δ_u degeneracy is not observed. On the other hand, experiments report nearly degenerate Σ_u^- states with excitation energies of 9.67 and 9.92 eV for the triplet and singlet states, respectively, in contrast with TD-DFT findings. This apparent failure of TD-DFT has been also reproduced elsewhere.[36,37] In a recent letter, it was shown that excited states such as N_2 Σ_u^- cannot be described by linear-response TD-DFT as their corresponding excitation energies do not correspond to poles of the response function.[38] TD-DFTB as an approximation to TD-DFT unavoidably inherits this issue and our correction is unable to fix it. However, it does break the wrong degeneracy of the triplet and singlet Δ_u states. For O_2, a similar degeneracy breaking of the transitions Σ_u^- and Δ_u within the corrected TD-DFTB can be observed. This is again in total agreement with first-principle results.

5.2. General Benchmark. To assess the general performance of the corrected TD-DFTB method in terms of vertical excitation energies, we have chosen a large benchmark set defined elsewhere,[39] which has been largely used during the past few years to test several density functionals[5−7,40−44] and DFT-based methods.[15,43−45] In particular, this set has been recently employed for the validation of TD-DFTB.[15] It covers $\pi \rightarrow \pi^*$, $n \rightarrow \pi^*$, and $\sigma \rightarrow \pi^*$ excitations for 28 organic compounds comprising unsaturated aliphatic hydrocarbons (group 1), aromatic hydrocarbons, and heterocycles (group 2), carbonyl compounds (group 3), and nucleobases (group 4), and intends to embrace the most important chromophores in organic photochemistry. For comparison we have calculated singlet

Table 2. Mean Signed Difference (MSD) and Root-Mean-Square Deviation (RMSD) of Singlet−Singlet Vertical Excitation Energies (in eV) Calculated within TD-DFTB and TD-DFT (along the Rows) with Respect to TD-PBE, TBE, and Experiment (along the Columns) Where Possible[a]

			TD-DFT				TD-DFTB	
					CAM-B3LYP			
		count	PBE	PBE0	RPA	TDA	new	old
				Group 1				
MSD	(PBE)	13					0.15	0.07
	(TBE)	13	−0.52	−0.09	0.26	0.49	−0.37	−0.45
	(exp.)	12	−0.35	0.05	0.34	0.63	−0.20	−0.26
RMS	(PBE)	13					0.28	0.25
	(TBE)	13	0.62	0.48	0.72	0.75	0.47	0.53
	(exp.)	12	0.56	0.56	0.80	0.90	0.39	0.46
				Group 2				
MSD	(PBE)	53					0.23	0.12
	(TBE)	53	−0.35	0.12	0.28	0.48	0.12	−0.23
	(exp.)	42	−0.06	0.38	0.44	0.76	0.13	0.02
RMS	(PBE)	53					0.41	0.36
	(TBE)	53	0.54	0.31	0.41	0.59	0.37	0.43
	(exp.)	42	0.39	0.49	0.59	0.85	0.35	0.34
				Group 3				
MSD	(PBE)	19					0.56	0.37
	(TBE)	19	−0.81	−0.21	0.02	0.12	−0.25	−0.44
	(exp.)	13	−0.67	−0.11	0.07	0.21	0.07	−0.08
RMS	(PBE)	19					1.06	0.93
	(TBE)	19	0.96	0.31	0.23	0.25	0.88	0.88
	(exp.)	13	0.88	0.27	0.17	0.31	0.70	0.64
				Group 4				
MSD	(PBE)	19					0.09	0.03
	(TBE)	19	−0.84	−0.06	0.28	0.39	−0.75	−0.81
	(exp.)	13	−0.51	0.18	0.34	0.65	−0.37	−0.29
RMS	(PBE)	19					0.32	0.30
	(TBE)	19	0.89	0.11	0.30	0.41	0.91	0.96
	(exp.)	13	0.63	0.30	0.45	0.70	0.61	0.64

[a]For the CAM-B3LYP functional, results are given as calculated with full TD-DFT, that is, following expression 19 (RPA) and under the Tamm−Damcoff approximation (TDA). In the MSD, the excitation energies of the assessed method were taken as the minuend, that is, a positive MSD denotes an overestimation with respect to the reference method.

and triplet vertical excitation energies at the TD-DFT level, employing three different density functionals: PBE, PBE0,[46,47] and CAM-B3LYP.[48] For the PBE and PBE0 cases, a TZP basis set was employed whereas we used 6-311G** basis functions for the range-separated-functional calculations. Given the known poor description of singlet−triplet (S−T) transition energies by TD-DFT due to triplet instabilities in the ground states,[49−51] we have also performed CAM-B3LYP/6-311G** calculations in the Tamm−Dancoff approximation[50] (TDA). The significant improvement of triplet states under the TDA was simultaneously shown by the groups of Tozer[52,53] and Brédas.[54] The TURBOMOLE package was used for those calculations involving the PBE and PBE0 functionals, whereas NWChem[55] was employed for CAM-B3LYP in both TD-DFT and TDA calculations. To disentangle the accuracy of the TD-DFTB approximation itself from the quality of DFTB ground state geometries, the same optimized structures were used along the benchmark. These geometries were previously obtained at a MP2 level.[39] In the Supporting Information, an extended table containing all our calculation results can be consulted. We include the KS energy difference of the corresponding dominant single-particle transition, which is useful for the analysis of the relative displacement of the excitation energies with respect to the KS energy difference as compared to ab initio TD-DFT at the PBE level (TD-PBE). Oscillator strengths are also given as another useful information. For further comparison, we also provide the theoretical best estimates (TBE) for this benchmark set, calculated at the CASPT2 level and reported by Schreiber and co-workers.[39] Reported experimental values for some vertical excitation energies are additionally given.

In Table 2 and 3, we present a statistical analysis of the collected data for the groups of compounds previously mentioned, for singlet-to-singlet and singlet-to-triplet transitions, respectively. In Table 4, the global statistics for the benchmark set is summarized. Here, the analysis has been also split into triplet and singlet excitations. The mean signed difference (MSD) as well as the root-mean-square deviation (RMS) of the TD-DFTB excitation energies with respect to the experiment, the TBE and TD-PBE are reported. Statistics on ab initio TD-DFT results are also provided to indicate its degree of correspondence with higher level of theory and experiment.

To assess the validity of our approximation, we focus on the comparison with the TD-PBE data set. It is important to recall that TD-DFTB parameters are calculated at this level of theory and the main aim of our approach is to improve its agreement with respect to the TD-DFT description. Since TD-DFT at the PBE level is of course an approximation itself, we are also

Table 3. Statistical Analysis of Singlet-Triplet Vertical Excitation Energies (in eV) Calculated within TD-DFTB and TD-DFT[a]

			TD-DFT				TD-DFTB	
					CAM-B3LYP			
		count	PBE	PBE0	RPA	TDA	new	old
				Group 1				
MSD	(PBE)	13					0.21	0.71
	(TBE)	13	−0.32	−0.60	−0.56	−0.13	−0.11	0.39
	(exp.)	11	−0.21	−0.54	−0.50	−0.03	0.00	0.54
RMS	(PBE)	13					0.32	0.78
	(TBE)	13	0.38	0.62	0.57	0.19	0.18	0.48
	(exp.)	11	0.25	0.56	0.53	0.10	0.21	0.61
				Group 2				
MSD	(PBE)	36					0.28	0.55
	(TBE)	36	−0.52	−0.41	−0.30	−0.13	−0.24	0.03
	(exp.)	12	−0.19	−0.18	−0.12	0.11	0.26	0.59
RMS	(PBE)	36					0.41	0.63
	(TBE)	36	0.63	0.48	0.42	0.26	0.41	0.45
	(exp.)	12	0.33	0.29	0.31	0.25	0.38	0.69
				Group 3				
MSD	(PBE)	14					0.42	0.79
	(TBE)	14	−0.61	−0.61	−0.52	−0.29	−0.20	0.17
	(exp.)	7	−0.53	−0.48	−0.35	−0.17	−0.13	0.27
RMS	(PBE)	14					0.47	0.83
	(TBE)	14	0.67	0.64	0.56	0.30	0.41	0.47
	(exp.)	7	0.57	0.52	0.44	0.24	0.39	0.57

[a]See Table 2 for details.

Table 4. Global Statistics for Vertical Excitation Energies (in eV) Calculated within TD-DFTB and TD-DFT[a]

			TD-DFT				TD-DFTB	
					CAM-B3LYP			
		count	PBE	PBE0	RPA	TDA	new	old
				Singlets				
MSD	(PBE)	104					0.25	0.14
	(TBE)	104	−0.55	0.00	0.23	0.40	−0.29	−0.40
	(exp.)	80	−0.28	0.22	0.34	0.63	−0.01	−0.12
RMS	(PBE)	104					0.57	0.50
	(TBE)	104	0.71	0.31	0.42	0.54	0.63	0.66
	(exp.)	80	0.56	0.45	0.55	0.77	0.48	0.47
				Triplets				
MSD	(PBE)	63					0.29	0.63
	(TBE)	63	−0.50	−0.49	−0.40	−0.16	−0.20	0.14
	(exp.)	30	−0.27	−0.38	−0.31	−0.01	0.07	0.50
RMS	(PBE)	63					0.40	0.71
	(TBE)	63	0.59	0.55	0.49	0.26	0.38	0.46
	(exp.)	30	0.38	0.46	0.43	0.21	0.33	0.63
				Total				
MSD	(PBE)	167					0.27	0.33
	(TBE)	167	−0.53	−0.19	−0.01	0.19	−0.26	−0.20
	(exp.)	110	−0.28	0.05	0.19	0.46	0.01	0.05
RMS	(PBE)	167					0.51	0.59
	(TBE)	167	0.67	0.42	0.44	0.45	0.55	0.59
	(exp.)	110	0.52	0.45	0.52	0.67	0.44	0.52

[a]See Table 2 for details.

interested in examining the accuracy of our method compared to a higher level of theory and experiment. In this case, we can benchmark both the traditional and corrected formalisms side by side with different TD-DFT approaches. It is worth mentioning that the subset of S−T excitations for which experimental observations are provided is around 50% smaller than the original set, but we consider it still suitable to perform a statistical analysis. The TBEs are available for the complete benchmark set on the other hand, and they are fairly close to their corresponding experimental values, with a RMS error of 0.24 eV for triplet states and 0.38 eV for singlet states. On average, both singlet and triplet TBEs are slightly overestimated (MSD = 0.15 and 0.20 eV, respectively),

which should be taken into account in the further analysis. Consistent with earlier studies,[5,6] TD-DFT excitation energies at the PBE level appear to be somewhat underestimated with regard to experimental findings as a general trend (MSD = −0.28 eV and −0.27 eV for singlet and triplet states, respectively). Opposed to this, with the incorporation of a fraction of exact exchange, singlet−singlet (S−S) excitation energies become overestimated, being in closer agreement with the TBEs. Especially, the PBE0 functional agrees significantly with a MSD = 0.00 and RMS of only 0.31 eV for S−S transitions. The TDA on the other hand shows a high overestimation of singlet energies, whereas returns the expected good accordance with TBEs and experiment for S−T excitations.

It can bee seen from Table 4 that with respect to TD-PBE, traditional TD-DFTB performs better for S−S than for S−T excitations. It should be pointed out, however, that S−T excitation energies are in better agreement with the TBE values than S−S energies. This has been noticed previously.[15] Nevertheless, compared to the collected experimental findings, S−S energies appear again to be more accurate than S−T energies. In fact, Table 4 shows a significant overestimation of triplet state energies compared to experiment (MSD = 0.50 eV) within traditional TD-DFTB. One of the main effects of our correction is the significant improvement of S−T excitation energies taking TD-PBE and experimental values as a reference. Within the refined formulation, the RMS error for this kind of transition is reduced by 0.3 eV with respect to both TD-PBE and experiment. More importantly, the RMS error with respect to the latter (0.33 eV) is slightly lower than that for TD-PBE itself (0.38 eV). This difference is yet increased if the functionals PBE0 (0.46 eV) and CAM-B3LYP (0.43 eV) are employed, and if the TBEs are taken as the reference, the RMS errors for TD-DFT S−T energies are even larger. Only the TDA clearly outperforms our method in this case. A similar accuracy for both TD-PBE and refined TD-DFTB can be seen for the first two groups of compounds, whereas for the third group the agreement with experimental data is somewhat better for our method (see Table 3). In addition, whereas Table 4 still indicates some overestimation of the corrected TD-DFTB results with respect to TD-PBE, the MSD of our refined approach compared to experiment becomes very small, which shows that the corrected S−T excitation energies are scattered around the experimental values. Specifically, in the group of aromatic hydrocarbons and heterocycles, transition energies are overestimated whereas there is some underestimation for the carbonyl compounds. Only with regard to TBE, the refined excitation energies appear to be underestimated for every group of compounds (see Table 3).

In contrast to the observations for S−T transitions, the traditional TD-DFTB method is, on average, in slightly better agreement with TD-PBE for the description of S−S excitations, compared to the new formulation. The RMS deviations of the corrected and noncorrected transition energies from TD-PBE values are in this case 0.57 and 0.50 eV, respectively (see top of Table 4). On the other hand, regarding the experimental references and the TBEs, both approaches perform with similar accuracy for this kind of transition. The refined formalism returns overestimated S−S excitation energies according to TD-PBE results, although with respect to experiment they are again spread around the reference values as can be seen from Table 2. In this case, the overestimation for the second group of compounds is compensated with the underestimation for the aliphatic hydrocarbons and the nucleobases, thus leading to an almost vanishing MSD (−0.01 eV). The results for the latter mentioned group of compounds are the least overestimated with respect to TD-PBE, with a MSD of only 0.09 eV. By contrast, the underestimation with respect to experiment is significant (MSD = −0.37 eV) and increases even more by taking the TBEs as the reference, for which the MSD amounts to −0.75 eV. For this group, the RMS error of TD-DFTB for singlet states with respect to TBEs is remarkably high (0.91 and 0.96 eV for the corrected and noncorrected approaches, respectively). The limited agreement between the TD-DFTB excitation energies of the nucleobases and their TBE counterparts has been already pointed out by Trani and co-workers.[15] However, it is necessary to notice that this failure should be rather attributed to TD-PBE itself and not to TD-DFTB as an approximation. In fact, the worst agreement between TD-PBE and TBE along the benchmark set is found for the carbonyl compounds and the nucleobases, with RMS errors of 0.96 and 0.89 eV, respectively. A very recent study by Foster and Wong indeed shows that conventional semilocal functionals fail in the description of the optical properties of nucleobases, while tuned range-separated functionals offer significant improvements.[56] This is evidenced by the good performance of CAM-B3LYP (see Table 2), whose RMS deviation from TBE is lowered to 0.30 eV. It should be indicated, however, that the best agreement with both experiment and TBEs is for the global hybrid functional PBE0, with RMS errors of 0.30 eV and only 0.11 eV, respectively. The enhancement of PBE0 over long-range corrected functionals for the description of these compounds has been previously pointed out by Jacquemin et al.[5]

The overall analysis (see bottom of Table 4) leads to somewhat smaller RMS errors for corrected TD-DFTB compared to the noncorrected formalism. It should be indicated, that despite the important improvements for the triplets states within the corrected formulation, the benchmark set for S−S excitations is comparatively larger, conceding more importance to this kind of transitions within the total balance. As a general behavior, it can be stated that TD-DFTB singlet excited states are shifted up in energy when the onsite correction is switched on. At the same time, the correction shifts triplet states down.

Let us investigate this trend in more detail. For local functionals, the TD-DFT coupling matrix leads to an upward shift of excitation energies with respect to Kohn−Sham energy differences for singlets and a downward shift for triplets. Ground state DFTB generally overestimates KS energy differences with respect to TD-PBE, due to the minimal basis set employed. In the original TD-DFTB, this error is partially compensated for singlet states, because the coupling matrix is underestimated with respect to first principles results. For triplet states the aforementioned errors do not compensate, but sum up, leading to strongly overestimated S−T energies. In the new approach, the underestimation of the coupling correction to KS energies is reduced, which leads to a widening of the singlet−triplet gap. Whereas S−T energies are now in much better accord with the TD-PBE reference, S−S energies are slightly overestimated. Given the fact that TD-PBE systematically underestimates S−S energies with respect to the experiment, the new formalism performs well for both S−S and S−T energies in this comparison.

We would now like to turn our attention to the overall accuracy of the singlet−triplet energy gap within the onsite correction. By inspection of Table 4, it should be noticed that with respect to every reference method, MSDs for corrected singlet and triplet states are similar, thus denoting a mean singlet−triplet gap in agreement with ab initio and experimental results. This is not the case for original TD-DFTB, where for the

most critical cases it gives large positive and negative MSDs for triplet and singlet states, respectively.

The singlet−triplet gap broadening under the onsite correction is particularly noticeable for $n \rightarrow \pi^*$ and $\sigma \rightarrow \pi^*$ excitations. The excitation energies for these transitions are either identically equal or (for few cases) very close to their corresponding KS energy differences at the noncorrected TD-DFTB level, resulting in degenerate or nearly degenerate singlet and triplet states (see Supporting Information). The only exception for this statement are the triplet B_{1u} states of tetrazine, for which an energy displacement occurs also for traditional TD-DFTB, although clearly underestimated with respect to the TD-PBE results. Within the onsite correction the excitation energies are either shifted down for triplets or shifted up for singlets with respect to the KS energy difference, leading to a singlet−triplet gap in accordance with the observations at the TD-DFT level. A similar degeneracy breaking was shown earlier for N_2. Also, in terms of oscillator strengths, these transitions are flawed in original TD-DFTB as they appear to be forbidden, in contradiction with the TD-DFT and TBE findings. The proposed correction returns nonzero oscillator strengths in agreement with more sophisticated calculations.

Considering only $n \rightarrow \pi^*$ and $\sigma \rightarrow \pi^*$ transitions, the RMS error of S−T excitation energies at the corrected (noncorrected) TD-DFTB level as compared to TD-PBE is 0.58 (0.82) eV. These kind of excitations are evidently difficult cases for the traditional formalism and an important improvement is obtained with the onsite correction, although the major quantitative enhancement of the latter approach is for S−T $\pi \rightarrow \pi^*$ transitions. Indeed, $n \rightarrow \pi^*$ and $\sigma \rightarrow \pi^*$ excitation energies are still strongly overestimated at the corrected TD-DFTB level with respect to TD-PBE, with MSD of 0.49 and 0.32 eV for triplet and singlet states, respectively. However, if we compare our findings with the TBEs, those are by contrast, significantly underestimated (MSD = −0.21 and −0.40 eV for S−T and S−S transitions, respectively) and the RMS deviations for both corrected and noncorrected formalisms are similar.

6. CONCLUSIONS

We have introduced and implemented new extensions of the time-dependent density functional based tight-binding (TD-DFTB) method. By taking the formalism beyond a mere Mulliken approximation, we have been able to surpass the inaccurate description of $n \rightarrow \pi^*$ and $\sigma \rightarrow \pi^*$ excitations within TD-DFTB. It was shown that particularly for the molecules O_2, NO, and N_2 these kind of transitions play an important role in the low energy optical spectra. Our refined formulation is in this case essential to obtain a qualitatively correct spectrum. Moreover, for the close-shell molecule N_2, the wrong $\sigma \rightarrow \pi^*$ triplet−singlet degeneracy encountered by using the original approach was successfully overcome. We additionally identified the erroneous degeneracy of $\pi \rightarrow \pi^*$ excitations with irreducible representations Σ^- and Δ for the investigated diatomic molecules as another failure of traditional TD-DFTB. The new formulation now delivers the correct behavior as compared to TD-DFT observations. Along with the qualitative improvement, a better numerical agreement with TD-DFT results can also be perceived for these systems.

To extend the analysis of the performance of our correction, we calculated the low-lying vertical excitation energies for a set of 28 benchmark compounds. We found a considerable improvement in the agreement with TD-PBE and experiment in terms of singlet−triplet excitation energies, whereas singlet−singlet energies have the same overall quality as in the traditional scheme. The accuracy of the corrected formalism is similar to that of TD-PBE for both triplet and singlet states, whereas the computational time of the former method is roughly 80 times smaller (see Figure 2).

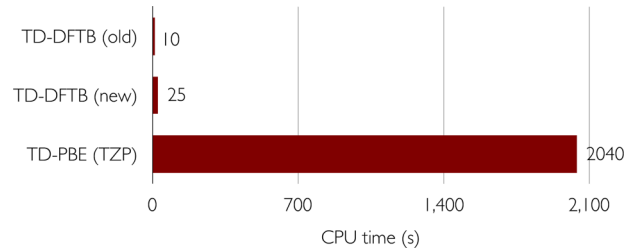

Figure 2. Total computational time required for calculating the low-lying excitation energies of a set of 28 molecules with traditional TD-DFTB (old), refined TD-DFTB (new), and full TD-DFT (PBE/TZP).

7. FUTURE PROSPECTS

The present work opens a variety of possibilities for further improvements and applications, which we briefly like to mention. First, the implementation of the onsite correction for the study of ground-state properties seems to be promising. In the past decade, DFTB has been greatly enhanced through several extensions. One of the most recent efforts to improve the method is based on a third-order expansion of the total energy.[57,58] However, our refinement indicates that there is still room for second-order corrections within DFTB, and its effects on different properties deserve a comprehensive investigation.

The low computational cost of the TD-DFTB approach makes it especially suitable for the study of photoinduced processes by means of quantum molecular dynamics simulations. In this regard, the effect of the onsite correction on the calculation of energy gradients is also under investigation.

Finally, we believe that the inclusion of hybrid functionals within TD-DFTB may improve the overall accuracy of the method and will allow for new promising applications. One of those is for example the development of an appropriate dressed TD-DFT-based formalism[45,59] for the description of double-excitations. Additionally, the implementation of range-separated functionals would make it possible to study charge-transfer excitations, which play a fundamental role in several photoreactions. The implementation of hybrid functionals for ground state DFTB,[60] as well as the development of a corresponding time-dependent formalism is currently under way.

APPENDIX A: PARAMETERS γ AND W

In spin-unrestricted DFTB, the appearing two-center integrals, Γ (eq 12), which depend on both the spin-up, $\rho_\uparrow$, and spin-down, $\rho_\downarrow$, charge densities are commonly split up into two terms, one depending on the total density, $\rho = \rho_\uparrow + \rho_\downarrow$, and the other on the spin density (or magnetization), $m = \rho_\uparrow - \rho_\downarrow$. In this manner, the method can be easily connected with its spin-restricted version by simply setting the latter integral to zero.

This transformation is done via a change of variables from the set $\{\rho_\uparrow,\rho_\downarrow\}$ to $\{\rho,m\}$; thus, the XC kernel can be expressed as follows:

$$\frac{\delta^2 E_{xc}[\rho_\uparrow, \rho_\downarrow]}{\delta\rho_\sigma(\mathbf{r})\delta\rho_\tau(\mathbf{r}')} = \frac{\delta^2 E_{xc}[\rho, m]}{\delta\rho(\mathbf{r})\delta\rho(\mathbf{r}')} + \delta_\sigma \frac{\delta^2 E_{xc}[\rho, m]}{\delta m(\mathbf{r})\delta\rho(\mathbf{r}')} + \delta_\tau \frac{\delta^2 E_{xc}[\rho, m]}{\delta\rho(\mathbf{r})\delta m(\mathbf{r}')} + \delta_\sigma\delta_\tau \frac{\delta^2 E_{xc}[\rho, m]}{\delta m(\mathbf{r})\delta m(\mathbf{r}')} \quad (34)$$

where $\delta_\sigma = 2\delta_{\uparrow\sigma} - 1$. By combining the Coulomb kernel with the second derivative of the XC energy with respect to total density (first term in eq 34), we obtain the γ functional introduced in the original SCC-DFTB paper,[61] whereas the last term is the kernel of the spin constants, W.[17] Thus, the functional Γ can be written as

$$\Gamma^{\sigma\tau}_{Al,Bl'} = \gamma_{Al,Bl'} + \delta_\sigma\delta_\tau\delta_{AB}W_{Al,l'} + 2\delta_\sigma\delta_{\sigma\tau}D_{Al,l'} \quad (35)$$

where

$$\gamma_{Al,Bl'} = \left\langle F_{Al} \left| \frac{1}{|\mathbf{r} - \mathbf{r}'|} + \frac{\delta^2 E_{xc}[\rho, m]}{\delta\rho(\mathbf{r})\delta\rho(\mathbf{r}')}\right|_{\rho_0,0} \right| F_{Bl'} \right\rangle$$

$$W_{Al,l'} = \left\langle F_{Al} \left| \frac{\delta^2 E_{xc}[\rho, m]}{\delta m(\mathbf{r})\delta m(\mathbf{r}')}\right|_{\rho_0,0} \right| F_{Bl'} \right\rangle$$

$$D_{Al,l'} = \left\langle F_{Al} \left| \frac{\delta^2 E_{xc}[\rho, m]}{\delta m(\mathbf{r})\delta\rho(\mathbf{r}')}\right|_{\rho_0,0} \right| F_{Bl'} \right\rangle \quad (36)$$

The derivatives of the XC functional are evaluated at the total density, ρ_0, and magnetization, $m = 0$, as the reference system is taken spin-unpolarized. The parameter D contains the mixed derivative with respect to ρ and m. If spin−orbit interactions are neglected, the XC functional must satisfy $E_{xc}[\rho,m] = E_{xc}[\rho,-m]$ and is therefore an even functional in m. This leads to $D = 0$ and the Γ parameters obtain their final form as in eq 13.

APPENDIX B: DFTB HAMILTONIAN IN TERMS OF MULLIKEN CHARGE AND SPIN POPULATIONS

The spin-unrestricted Hamiltonian obtained in the original work of Köhler et al.[17] can be derived from the formalism presented here by substituting the KS density matrix fluctuation, $\Delta P^\tau_{uv} = n_{u\tau}\delta_{uv} - P^{0,\tau}_{uv}$ and the expression 15 for the $\bar{\mathbf{K}}$ matrix in eq 30:

$$H_{st\sigma} = H^0_{st\sigma} + \sum_\tau \sum_{ACll''} \Gamma^{\sigma\tau}_{Al,Cl''} q^{st\sigma}_{Al} \left(\sum_u n_{u\tau} q^{uu\tau}_{Cl''} - \sum_{uv} P^{0,\tau}_{uv} q^{uv\tau}_{Cl''} \right) \quad (37)$$

By using definition 10, the sum,

$$\sum_u n_{u\tau} q^{uu\tau}_{Cl''} = \sum_u n_{u\tau} \sum_{\kappa\in C,l''} P^{uu\tau}_{\kappa\kappa} = \sum_u n_{u\tau} \sum_{\kappa\in C,l''} \sum_\lambda c^\tau_{\kappa u} c^\tau_{\lambda u} S_{\kappa\lambda} \equiv q^\tau_{Cl''} \quad (38)$$

gives the Mulliken charge population for the orbitals with quantum number l'' and spin τ at center C, whereas the sum,

$$\sum_{uv} P^{0,\tau}_{uv} q^{uv\tau}_{Cl''} = \frac{1}{2} \sum_{uv} P^{0,\tau}_{uv} \sum_{\kappa\in Cl''} \sum_\lambda S_{\kappa\lambda} (c^\tau_{\kappa u} c^\tau_{\lambda v} + c^\tau_{\kappa v} c^\tau_{\lambda u}) = \sum_{\kappa\in Cl''} n^0_{\kappa\tau} \quad (39)$$

gives the population for the aforementioned orbitals corresponding to the reference system. For the latter sum, the identity, $\Sigma_{uv} C^\tau_{ku} P^{0\tau}_{uv} C^\tau_{\lambda u} = n^0_{k\tau}\delta_{k\lambda}$, was additionally employed. Making use again of definition 10 for $q^{st\sigma}_{Al}$ in eq 37, leads to the following expression for the KS Hamiltonian:

$$H_{st\sigma} = \sum_{\mu\nu} c^\sigma_{\mu s} c^\sigma_{\nu t} H_{\mu\nu\sigma} \quad (40)$$

with

$$H_{\mu\nu\sigma} = H^0_{\mu\nu\sigma} + \frac{1}{2} S_{\mu\nu} \sum_\tau \sum_{Cl''} (\Gamma^{\sigma\tau}_{Al,Cl''} + \Gamma^{\sigma\tau}_{Bl',Cl''}) \Delta q^\tau_{Cl''} \quad (41)$$

In eq 41, A and l (B and l'') denote, respectively, the center and angular quantum number of AO ϕ_μ (ϕ_ν), and the spin-dependent charge fluctuation, $\Delta q^\tau_{Cl''} = q^\tau_{Cl''} - \Sigma_{k\in Cl''} n^0_{k\tau}$.

By using eq 13, the Hamiltonian matrix elements, $H_{\mu\nu\sigma}$, can be finally expressed as

$$H_{\mu\nu\sigma} = H^0_{\mu\nu\sigma} + \frac{1}{2} S_{\mu\nu} \sum_{Cl''} (\gamma_{Al,Cl''} + \gamma_{Bl',Cl''}) \Delta q_{Cl''} + \frac{1}{2}\delta_\sigma S_{\mu\nu} \sum_{l''} (W_{Al,l''} \Delta m_{Al''} + W_{Bl',l''} \Delta m_{Bl''}) \quad (42)$$

where $\Delta q_{Cl''} = \Delta q^\uparrow_{Cl''} + \Delta q^\downarrow_{Cl''}$ and $\Delta m_{Cl''} = \Delta q^\uparrow_{Cl''} - \Delta q^\downarrow_{Cl''}$ are the fluctuations of the l-resolved atomic charge and spin populations, respectively.

APPENDIX C: ONSITE CORRECTION TO THE TOTAL ENERGY

Let $\{\phi_\alpha\}$ and $\{\phi_\beta\}$ be a complete set of real orbitals placed at atom A and B, respectively. The orbitals are assumed to be orthonormal within each set, while the overlap between orbitals on different atoms is given by $S_{\alpha\beta}$. Let also $\mu \in A, \nu \in B, \kappa \in C$ and $\lambda \in D$ unless otherwise specified. Then, the orbitals ϕ_μ and ϕ_ν can be expanded as

$$\phi_\mu(\mathbf{r}) = \sum_{\beta\in B} S_{\beta\mu}\phi_\beta(\mathbf{r}),\ \phi_\nu(\mathbf{r}) = \sum_{\alpha\in A} S_{\alpha\nu}\phi_\alpha(\mathbf{r}) \quad (43)$$

Hence, the orbital product can be expressed as

$$\phi_\mu(\mathbf{r})\phi_\nu(\mathbf{r}) = \frac{1}{2}\left(\sum_{\alpha\in A} S_{\alpha\nu}\phi_\alpha(\mathbf{r})\phi_\mu(\mathbf{r}) + \sum_{\beta\in B} S_{\beta\mu}\phi_\beta(\mathbf{r})\phi_\nu(\mathbf{r}) \right) \quad (44)$$

and more conveniently as

$$\phi_\mu(\mathbf{r})\phi_\nu(\mathbf{r}) = \frac{1}{2} S_{\mu\nu}(|\phi_\mu(\mathbf{r})|^2 + |\phi_\nu(\mathbf{r})|^2) + \frac{1}{2}\left(\sum_{\alpha\in A}^{\alpha\neq\mu} S_{\alpha\nu}\phi_\alpha(\mathbf{r})\phi_\mu(\mathbf{r}) + \sum_{\beta\in B}^{\beta\neq\nu} S_{\beta\mu}\phi_\beta(\mathbf{r})\phi_\nu(\mathbf{r}) \right) \quad (45)$$

where the first term accounts for the Mulliken approach. Let us now denote with $(\mu\nu|\kappa\lambda)$ a two-electron integral with an arbitrary kernel. Using eq 45, the integrals $(\mu\nu|\kappa\lambda)$ can then be expanded as

dx.doi.org/10.1021/ct400123t | J. Chem. Theory Comput. 2013, 9, 4901−4914

$$
\begin{aligned}
(\mu\nu|\kappa\lambda) = {} & \frac{1}{4}S_{\mu\nu}S_{\kappa\lambda}[(\mu\mu|\kappa\kappa) + (\mu\mu|\lambda\lambda) + (\nu\nu|\kappa\kappa) + (\nu\nu|\lambda\lambda)] \\
& + \frac{1}{4}S_{\mu\nu}\left(\sum_{\gamma\in C}^{\gamma\neq\kappa} S_{\gamma\lambda}[(\mu\mu|\kappa\gamma) + (\nu\nu|\kappa\gamma)] \right. \\
& \left. + \sum_{\delta\in D}^{\delta\neq\lambda} S_{\delta\kappa}[(\mu\mu|\delta\lambda) + (\nu\nu|\delta\lambda)]\right) \\
& + \frac{1}{4}S_{\kappa\lambda}\left(\sum_{\alpha\in A}^{\alpha\neq\mu} S_{\alpha\nu}[(\mu\alpha|\kappa\kappa) + (\mu\alpha|\lambda\lambda)] \right. \\
& \left. + \sum_{\beta\in B}^{\beta\neq\nu} S_{\beta\mu}[(\beta\nu|\kappa\kappa) + (\beta\nu|\lambda\lambda)]\right) \\
& + \frac{1}{4}\left(\sum_{\alpha\in A}^{\alpha\neq\mu}\sum_{\gamma\in C}^{\gamma\neq\kappa} S_{\alpha\nu}S_{\gamma\lambda}(\mu\alpha|\kappa\gamma) + \sum_{\alpha\in A}^{\alpha\neq\mu}\sum_{\delta\in D}^{\delta\neq\lambda} S_{\alpha\nu}S_{\delta\kappa}(\mu\alpha|\delta\lambda)\right) \\
& + \frac{1}{4}\left(\sum_{\beta\in B}^{\beta\neq\nu}\sum_{\gamma\in C}^{\gamma\neq\kappa} S_{\beta\mu}S_{\gamma\lambda}(\beta\nu|\kappa\gamma) + \sum_{\beta\in B}^{\beta\neq\nu}\sum_{\delta\in D}^{\delta\neq\lambda} S_{\beta\mu}S_{\delta\kappa}(\beta\nu|\delta\lambda)\right)
\end{aligned}
\tag{46}
$$

Note that the expression eq 46 is exact as long as the AO sets $\{\phi_\alpha\}$, $\{\phi_\beta\}$, $\{\phi_\gamma\}$, and $\{\phi_\delta\}$ are complete. The first line in eq 46 contains the leading terms, which include Coulomb-like integrals. Truncation of the expansion up to the first line accounts for the Mulliken approach. A next level of approximation demands the inclusion of fully onsite exchange-like integrals, that is, $(\mu\nu|\mu\nu)$, with $\mu,\nu \in A$ and $\mu \neq \nu$. At this level of theory the general four-center integrals can be expressed as

$$
(\mu\nu|\kappa\lambda) \approx (\mu\nu|\kappa\lambda)_{\text{mull}} + (\mu\nu|\kappa\lambda)_{\text{ons}} \tag{47}
$$

where

$$
(\mu\nu|\kappa\lambda)_{\text{mull}} = \frac{1}{4}S_{\mu\nu}S_{\kappa\lambda}[(\mu\mu|\kappa\kappa) + (\mu\mu|\lambda\lambda) + (\nu\nu|\kappa\kappa) + (\nu\nu|\lambda\lambda)] \tag{48}
$$

and

$$
\begin{aligned}
(\mu\nu|\kappa\lambda)_{\text{ons}} = {} & \frac{1}{4}\sum_{\alpha\in A}^{\alpha\neq\mu} S_{\alpha\nu}S_{\alpha\lambda}(\mu\alpha|\mu\alpha)\delta_{\mu\kappa} + \frac{1}{4}\sum_{\alpha\in A}^{\alpha\neq\mu} S_{\alpha\nu}S_{\alpha\kappa}(\mu\alpha|\mu\alpha)\delta_{\mu\lambda} \\
& + \frac{1}{4}\sum_{\beta\in B}^{\beta\neq\nu} S_{\beta\mu}S_{\beta\lambda}(\beta\nu|\beta\nu)\delta_{\nu\kappa} + \frac{1}{4}\sum_{\beta\in B}^{\beta\neq\nu} S_{\beta\mu}S_{\beta\kappa}(\beta\nu|\beta\nu)\delta_{\nu\lambda} \\
& + \frac{1}{4}S_{\kappa\nu}S_{\mu\lambda}(\mu\kappa|\mu\kappa)\delta_{AC}(1-\delta_{\mu\kappa}) + \frac{1}{4}S_{\lambda\nu}S_{\mu\kappa}(\mu\lambda|\mu\lambda) \\
& \times \delta_{AD}(1-\delta_{\mu\lambda}) + \frac{1}{4}S_{\kappa\mu}S_{\nu\lambda}(\nu\kappa|\nu\kappa)\delta_{BC}(1-\delta_{\nu\kappa}) \\
& + \frac{1}{4}S_{\lambda\mu}S_{\nu\kappa}(\nu\lambda|\nu\lambda)\delta_{BD}(1-\delta_{\nu\lambda})
\end{aligned}
\tag{49}
$$

The contribution to the DFTB total energy originating from this correction is written as

$$
E_{\text{ons}} = \frac{1}{2}\sum_{\sigma\tau}\sum_{\mu\nu\kappa\lambda} \Delta P^{\sigma}_{\mu\nu}(\mu\nu|f^{\text{hxc}}_{\rho_\sigma\rho_\tau}[\rho_0]|\kappa\lambda)_{\text{ons}}\Delta P^{\tau}_{\kappa\lambda} \tag{50}
$$

After substituting eq 49 in eq 50, we finally arrive at

$$
E_{\text{ons}} = \sum_{\sigma\tau}\sum_{A}\sum_{\mu\nu\in A}^{\mu\neq\nu} \Delta\tilde{P}^{\sigma}_{\mu\nu}(\mu\nu|f^{\text{hxc}}_{\rho_\sigma\rho_\tau}[\rho_0]|\mu\nu)\Delta\tilde{P}^{\tau}_{\mu\nu} \tag{51}
$$

where $\tilde{P}^{\sigma}_{\mu\nu}$ are the matrix elements of the dual density matrix defined in eq 8.

APPENDIX D: ONSITE CORRECTION TO DIPOLE MATRIX ELEMENTS

To derive an expression for the KS dipole matrix elements, we expand the KS orbitals into a set of localized atom-centered AO, $\psi_{s\sigma} = \Sigma_\mu c^{\sigma}_{\mu s}\phi_\mu$. Thus, the dipole matrix elements read

$$
\langle\psi_{s\sigma}|\hat{\mathbf{r}}|\psi_{t\sigma}\rangle = \sum_{\mu\nu} c^{\sigma}_{\mu s}\langle\mu|\hat{\mathbf{r}}|\nu\rangle c^{\sigma}_{\nu t} \tag{52}
$$

Let $\mu \in A$ and $\nu \in B$ unless otherwise indicated. Using the orbital product expansion eq 45, the AO dipole matrix elements, $\langle\mu|\hat{\mathbf{r}}|\nu\rangle$, can be expressed as follows,

$$
\langle\mu|\hat{\mathbf{r}}|\nu\rangle = \frac{1}{2}S_{\mu\nu}(\mathbf{R}_A + \mathbf{R}_B) + \frac{1}{2}\left(\sum_{\alpha\in A}^{\alpha\neq\mu} S_{\alpha\nu}\langle\alpha|\hat{\mathbf{r}}|\mu\rangle + \sum_{\beta\in B}^{\beta\neq\nu} S_{\beta\mu}\langle\beta|\hat{\mathbf{r}}|\nu\rangle\right) \tag{53}
$$

where $\mathbf{R}_A = \langle\mu|\hat{\mathbf{r}}|\mu\rangle$ and $\mathbf{R}_B = \langle\nu|\hat{\mathbf{r}}|\nu\rangle$ denote the positions of centers A and B, respectively. After substituting eq 53 in eq 52, we finally have

$$
\langle\psi_{s\sigma}|\hat{\mathbf{r}}|\psi_{t\sigma}\rangle = \sum_{A}\mathbf{R}_A q^{st\sigma}_{A} + \sum_{A}\sum_{\mu\nu\in A}^{\mu\neq\nu} P^{st\sigma}_{\mu\nu}\langle\mu|\hat{\mathbf{r}}|\nu\rangle \tag{54}
$$

where the definition eq 10 was additionally employed.

APPENDIX E: EVALUATION OF ONSITE PARAMETERS

For the evaluation of the one-center integrals required in our correction, the kernel is first separated into Hartree and XC contributions:

$$
(\mu\nu|f^{\text{hxc}}_{\rho_\sigma\rho_\tau}[\rho_0]|\mu\nu) = (\mu\nu|f^{\text{h}}|\mu\nu) + (\mu\nu|f^{\text{xc}}_{\rho_\sigma\rho_\tau}[\rho_0]|\mu\nu) \tag{55}
$$

For the evaluation of the Hartree component we use the method introduced by Becke,[62] adapted for one-center integrals with integrands separable into radial and angular parts. Let us denote with letter g the atomic orbital products,

$$
g_{\mu\nu}(\mathbf{r}) = \phi_\mu(\mathbf{r})\phi_\nu(\mathbf{r}) = R_{\mu\nu}(r)Y_\mu(\Omega)Y_\nu(\Omega) \tag{56}
$$

where Y are real spherical harmonics and the function $R_{\mu\nu}$ is the radial part of $g_{\mu\nu}$. Then, we can write the Hartree integral as follows:

$$
(\mu\nu|f^{h}|\mu\nu) = \int g_{\mu\nu}(\mathbf{r})V_{\mu\nu}(\mathbf{r})\mathrm{d}\mathbf{r} \tag{57}
$$

where the potential $V_{\mu\nu}$ is defined as

$$
V_{\mu\nu}(\mathbf{r}) = \int\frac{g_{\mu\nu}(\mathbf{r}')}{|\mathbf{r}-\mathbf{r}'|}\mathrm{d}\mathbf{r}' \tag{58}
$$

Next, we expand $g_{\mu\nu}$ and $V_{\mu\nu}$ into spherical harmonics,

$$
\begin{aligned}
g_{\mu\nu}(\mathbf{r}) &= \sum_{lm}\left[\int g_{\mu\nu}(\mathbf{r})Y_{lm}(\Omega')d\Omega'\right]Y_{lm}(\Omega) \\
&= \sum_{lm} G(\mu,\nu,lm)R_{\mu\nu}(r)Y_{lm}(\Omega)
\end{aligned}
\tag{59}
$$

$$
V_{\mu\nu}(\mathbf{r}) = \sum_{lm} r^{-1}V^{lm}_{\mu\nu}(r)Y_{lm}(\Omega) \tag{60}
$$

where $G(\mu,\nu,lm) = \int Y_\mu(\Omega)Y_\nu(\Omega)Y_{lm}(\Omega)d\Omega$ are real Gaunt coefficients and $V^{lm}_{\mu\nu}$ are radial functions. The separation of variables described in eq 60 can be demonstrated by writing the coulomb kernel in terms of spherical harmonics,

dx.doi.org/10.1021/ct400123t | J. Chem. Theory Comput. 2013, 9, 4901−4914

$$\frac{1}{|\mathbf{r}-\mathbf{r}'|} = \sum_{lm} R_l^{>} R_l^{<} Y_{lm}(\Omega) Y_{lm}(\Omega') \tag{61}$$

$$R_l^{>} = \max(r, r')^{-l-1} \sqrt{\frac{4\pi}{2l+1}} \tag{62}$$

$$R_l^{<} = \min(r, r')^{l} \sqrt{\frac{4\pi}{2l+1}} \tag{63}$$

which is achieved via a Legendre expansion followed by use of the addition theorem for spherical harmonics. By substituting eq 61 and eq 59 in eq 58 and integrating over the angular coordinates, one obtains,

$$V_{\mu\nu}(\mathbf{r}) = \sum_{lm} G(\mu, \nu, lm) Y_{lm}(\Omega) \frac{4\pi}{2l+1} \times \left[\frac{1}{r^{l+1}} \int_0^r r'^{l+2} R_{\mu\nu}(r') \mathrm{d}r' + r^l \int_r^\infty r'^{-l+1} R_{\mu\nu}(r') \mathrm{d}r' \right] \tag{64}$$

which has the same form as in eq 60.

To determine the potentials $V_{\mu\nu}^{lm}$ we make use of the Poisson equation, $\nabla^2 V_{\mu\nu} = -4\pi g_{\mu\nu}$, which leads to the following radial equations,

$$\frac{d^2 V_{\mu\nu}^{lm}(r)}{dr^2} - \frac{l(l+1)}{r^2} V_{\mu\nu}^{lm}(r) = -4\pi r G(\mu, \nu, lm) R_{\mu\nu}(r) \tag{65}$$

from which $V_{\mu\nu}^{lm}$ is obtained by using finite difference method with the same boundary values as in ref 62. Finally, by substitution of eqs 59 and 60 in eq 57 and integrating the angular part, the Hartree integral reads,

$$(\mu\nu|f^h|\mu\nu) = \int r R_{\mu\nu}(r) \sum_{lm} G(\mu, \nu, lm) V_{\mu\nu}^{lm}(r) \mathrm{d}r \tag{66}$$

The radial integration is performed using Tschebyshev quadrature with a grid of 400 points, which provides, at least, eight digits of precision. For a given atomic orbitals, ϕ_μ and ϕ_ν, the maximal l in the above expansion is determined by selection rules for Gaunt coefficients.[63]

The evaluation of the XC component is carried out by writing the two-electron integral as in eqs 8 and 9 of ref 64. Next, the separation of the atomic orbitals into radially dependent and angularly dependent portions, as well as the expansion of the AO products into spherical harmonics is carried out as above. The angular part, containing products of spherical harmonics and of their gradients is then expressed in terms of Gaunt coefficients. The radial integration is carried out as for the Hartree component. The **libxc** library (version 1.2.0)[65] was employed for the evaluation of the partial derivatives of the XC functional.

■ ASSOCIATED CONTENT

Supporting Information

In a separate PDF document we provide the vertical excitation energies and oscillator strengths for the chosen benchmark set, obtained with TD-DFTB and TD-DFT. This information is available free of charge via the Internet at http://pubs.acs.org.

■ AUTHOR INFORMATION

Corresponding Author

*E-mail: adrielg@bccms.uni-bremen.de.

Notes

The authors declare no competing financial interest.

■ ACKNOWLEDGMENTS

Financial support from the Deutsche Forschungsgemeinschaft (GRK 1570 and SPP 1243) and the DAAD is gratefully acknowledged.

■ REFERENCES

(1) Runge, E.; Gross, E. K. U. *Phys. Rev. Lett.* **1984**, *52*, 997−1000.
(2) Casida, M. E.; Huix-Rotllant, M. *Annu. Rev. Phys. Chem.* **2012**, *63*, 287−323.
(3) Burke, K. *J. Chem. Phys.* **2012**, *136*, 150901.
(4) Ullrich, C. *Time-Dependent Density-Functional Theory: Concepts and Applications*; Oxford University Press, New York, 2012.
(5) Jacquemin, D.; Wathelet, V.; Perpete, E. A.; Adamo, C. *J. Chem. Theory Comput.* **2009**, *5*, 2420−2435.
(6) Jacquemin, D.; Perpete, E. A.; Ciofini, I.; Adamo, C. *J. Chem. Theory Comput.* **2010**, *6*, 1532−1537.
(7) Jacquemin, D.; Perpete, E. A.; Ciofini, I.; Adamo, C.; Valero, R.; Zhao, Y.; Truhlar, D. G. *J. Chem. Theory Comput.* **2010**, *6*, 2071−2085.
(8) Niehaus, T. A.; Suhai, S.; Della Sala, F.; Lugli, P.; Elstner, M.; Seifert, G.; Frauenheim, T. *Phys. Rev. B* **2001**, *63*, 085108.
(9) Heringer, D.; Niehaus, T. A.; Wanko, M.; Frauenheim, T. *J. Comput. Chem.* **2007**, *28*, 2589−2601.
(10) Yam, C. Y.; Yokojima, S.; Chen, G. H. *Phys. Rev. B* **2003**, *68*, 153105.
(11) Niehaus, T. A.; Heringer, D.; Torralva, B.; Frauenheim, T. *Eur. Phys. J. D* **2005**, *35*, 467−477.
(12) Mitric, R.; Werner, U.; Wohlgemuth, M.; Seifert, G.; Bonacic-Koutecký, V. *J. Phys. Chem. A* **2009**, *113*, 12700−12705.
(13) Jakowski, J.; Irle, S.; Morokuma, K. *Phys. Chem. Chem. Phys.* **2012**, *14*, 6273−6279.
(14) Wang, Y.; Yam, C.-Y.; Frauenheim, T.; Chen, G.; Niehaus, T. *Chem. Phys.* **2011**, *391*, 69−77.
(15) Trani, F.; Scalmani, G.; Zheng, G.; Carnimeo, I.; Frisch, M.; Barone, V. *J. Chem. Theory Comput.* **2011**, *7*, 3304−3313.
(16) Niehaus, T. A. *J. Mol. Struct.: THEOCHEM* **2009**, *914*, 38−49.
(17) Köhler, C.; Seifert, G.; Gerstmann, U.; Elstner, M.; Overhof, H.; Frauenheim, T. *Phys. Chem. Chem. Phys.* **2001**, *3*, 5109−5114.
(18) Frauenheim, T.; Seifert, G.; Elstner, M.; Niehaus, T.; Kohler, C.; Amkreutz, M.; Sternberg, M.; Hajnal, Z.; Di Carlo, A.; Suhai, S. *J. Phys.: Condens. Matter* **2002**, *14*, 3015−3047.
(19) Han, M. J.; Ozaki, T.; Yu, J. *Phys. Rev. B* **2006**, *73*, 045110.
(20) Casida, M. E. Time-dependent Density Functional Response Theory for Molecules. In *Recent Advances in Density Functional Methods, Part I*; Chong, D., Ed.; World Scientific: Singapore, 1995; pp 155−192.
(21) See ref 60 for an extension of DFTB to general hybrid functionals.
(22) The parameter W is termed M in ref 8.
(23) Pople, J. A.; Beveridge, D. L.; Dobosh, P. A. *J. Chem. Phys.* **1967**, *47*, 2026−2033.
(24) Pople, J. A.; Santry, D. P.; Segal, G. A. *J. Chem. Phys.* **1965**, *43*, S129−s135.
(25) Figeys, H.; Geerlings, P.; Van Alsenoy, C. *Int. J. Quantum Chem.* **1977**, *11*, 705−713.
(26) For p-type orbitals we have for example $(pp|f^{hxc}_{\rho\sigma\rho\tau}[\rho_0]|pp) = \Gamma^{\sigma\tau}_{Ap,Ap} + 4/3(pp'|f^{hxc}_{\rho\sigma\rho\tau}[\rho_0]|pp')$ and $(pp|f^{hxc}_{\rho\sigma\rho\tau}[\rho_0]|p'p') = \Gamma^{\sigma\tau}_{Ap,Ap} - 2/3(pp'|f^{hxc}_{\rho\sigma\rho\tau}[\rho_0]|pp')$. Here the Γ-parameters are obtained from total energy derivatives, while the exchange integrals are evaluated directly from the wave function.
(27) Perdew, J.; Burke, K.; Ernzerhof, M. *Phys. Rev. Lett.* **1996**, *77*, 3865−3868.
(28) The employed Slater-Koster tables (mio-0−1[61,66]) are available online at http://www.dftb.org/parameters/download/mio/mio_0_1 (accessed May 30, 2013).
(29) Aradi, B.; Hourahine, B.; Frauenheim, T. *J. Phys. Chem. A* **2007**, *111*, 5678−5684.
(30) Casida, M. E. *J. Mol. Struct.: THEOCHEM* **2009**, *914*, 3−18.

(31) This expression is in accordance with the simplified characterization of the many body excited state in terms of singly excited Slater determinants given by Casida.[20] A more rigorous formula for $\langle S^2 \rangle$ can be found in ref 67. As our goal is just a rough assignment of the multiplicity and the detection of spin-contaminated states, we work with the simpler form here.
(32) *TURBOMOLE* V6.4 2012, a development of University of Karlsruhe and Forschungszentrum Karlsruhe GmbH, 1989−2007, TURBOMOLE GmbH, since 2007; available from http://www.turbomole.com (accessed May 30, 2013).
(33) Oddershede, J.; Gruener, N. E.; Diercksen, G. H. F. *Chem. Phys.* **1985**, *97*, 303−310.
(34) Krupenie, P. H. *J. Phys. Chem. Ref. Data* **1972**, *1* (2), 423−534.
(35) The *y*-axis represents the molar extinction coefficient, $\varepsilon = \sum_I \varepsilon_I$. For its calculation we use the relationship, $f_I = C\int \varepsilon_I(\omega)\mathrm{d}\omega$,[68] where f_I is the oscillator strength related to excitation *I*, $C = 3.5 \times 10^{-5}$ M cm/eV and the energy, ω, is given in eV. By using Lorentzian functions for the spectral broadening, the extinction coefficient can then be written as, $\varepsilon(\omega) = \Sigma_I(f_I/C\pi)((\Gamma/2)/((\omega - \omega_I)_2 + (\Gamma/2)^2))$. The parameter Γ specifying the function width was set to 0.5 eV.
(36) Grabo, T.; Petersilka, M.; Gross, E. K. U. *J. Mol. Struct.: THEOCHEM* **2000**, *501*−*502*, 353−367.
(37) Bauernschmitt, R.; Ahlrichs, R. *Chem. Phys. Lett.* **1996**, *256*, 454−464.
(38) Hesselmann, A.; Goerling, A. *Phys. Rev. Lett.* **2009**, *102*, 233003.
(39) Schreiber, M.; Silva-Junior, M.; Sauer, S.; Thiel, W. *J. Chem. Phys.* **2008**, *128*, 134110.
(40) Peverati, R.; Truhlar, D. G. *Phys. Chem. Chem. Phys.* **2012**, *14*, 11363−11370.
(41) Goerigk, L.; Moellmann, J.; Grimme, S. *Phys. Chem. Chem. Phys.* **2009**, *11*, 4611−4620.
(42) Mardirossian, N.; Parkhill, J. A.; Head-Gordon, M. *Phys. Chem. Chem. Phys.* **2011**, *13*, 19325−19337.
(43) Sala, F. D.; Fabiano, E. *Chem. Phys.* **2011**, *391*, 19−26.
(44) Silva-Junior, M. R.; Schreiber, M.; Sauer, S. P. A.; Thiel, W. *J. Chem. Phys.* **2008**, *129*, 104103.
(45) Huix-Rotllant, M.; Ipatov, A.; Rubio, A.; Casida, M. E. *Chem. Phys.* **2011**, *391*, 120−129.
(46) Adamo, C.; Barone, V. *J. Chem. Phys.* **1999**, *110*, 6158−6170.
(47) Ernzerhof, M.; Scuseria, G. E. *J. Chem. Phys.* **1999**, *110*, 5029−5036.
(48) Yanai, T.; Tew, D. P.; Handy, N. C. *Chem. Phys. Lett.* **2004**, *393*, 51−57.
(49) Dreuw, A.; Head-Gordon, M. *Chem. Rev.* **2005**, *105*, 4009−4037.
(50) Hirata, S.; Head-Gordon, M. *Chem. Phys. Lett.* **1999**, *314*, 291−299.
(51) Casida, M. E.; Gutierrez, F.; Guan, J. G.; Gadea, F. X.; Salahub, D.; Daudey, J. P. *J. Chem. Phys.* **2000**, *113*, 7062−7071.
(52) Peach, M. J. G.; Williamson, M. J.; Tozer, D. J. *J. Chem. Theory Comput.* **2011**, *7*, 3578−3585.
(53) Peach, M. J. G.; Tozer, D. J. *J. Phys. Chem. A* **2012**, *116*, 9783−9789.
(54) Sears, J. S.; Koerzdoerfer, T.; Zhang, C.-R.; Bredas, J.-L. *J. Chem. Phy.* **2011**, *135*, 151103.
(55) Valiev, M.; Bylaska, E.; Govind, N.; Kowalski, K.; Straatsma, T.; Dam, H. V.; Wang, D.; Nieplocha, J.; Apra, E.; Windus, T.; de Jong, W. *Comput. Phys. Commun.* **2010**, *181*, 1477−1489.
(56) Foster, M. E.; Wong, B. M. *J. Chem. Theory Comput.* **2012**, *8*, 2682−2687.
(57) Yang, Yu, H.; York, D.; Cui, Q.; Elstner, M. *J. Phys. Chem. A* **2007**, *111*, 10861−10873.
(58) Gaus, M.; Cui, Q.; Elstner, M. *J. Chem. Theory Comput.* **2011**, *7*, 931−948.
(59) Maitra, N. T.; Zhang, F.; Cave, R. J.; Burke, K. *J. Chem. Phys.* **2004**, *120*, 5932−5937.
(60) Niehaus, T.; Della Sala, F. *Phys. Status Solidi B* **2012**, *249*, 237−244.
(61) Elstner, M.; Porezag, D.; Jungnickel, G.; Elsner, J.; Haugk, M.; Frauenheim, T.; Suhai, S.; Seifert, G. *Phys. Rev. B* **1998**, *58*, 7260−7268.
(62) Becke, A. D. *J. Chem. Phys.* **1988**, *88*, 2547−2553.
(63) Homeier, H. H. H.; Steinborn, E. O. *J. Mol. Struct.: THEOCHEM* **1996**, *368*, 31−37.
(64) Hirata, S.; Head-Gordon, M. *Chem. Phys. Lett.* **1999**, *302*, 375−382.
(65) Marques, M. A. L. *Comput. Phys. Commun.* **2012**, *183*, 2272−2281.
(66) Niehaus, T. A.; Elstner, M.; Frauenheim, T.; Suhai, S. *J. Mol. Struct.: THEOCHEM* **2001**, *541*, 185−194.
(67) Ipatov, A.; Cordova, F.; Doriol, L. J.; Casida, M. E. *J. Mol. Struct.: THEOCHEM* **2009**, *914*, 60−73.
(68) Turro, N. J.; Ramamurthy, V.; Scaiano, J. C. *In Principles of Molecular Photochemistry: An Introduction*, 1st ed.; Stiefel, J., Ed.; University Science Books: Sausalito, CA, 2009; pp 195−196.